Molecular Biology Reports (2018) 45:433–443
https://doi.org/10.1007/s11033-018-4179-7

ORIGINAL ARTICLE

Molecular identification and transcriptional regulation of porcine *IFIT2* gene

Xiuqin Yang[1] · Xiaoyan Jing[1] · Yanfang Song[1] · Caixia Zhang[1] · Di Liu[2]

Received: 6 October 2017 / Accepted: 2 April 2018 / Published online: 6 April 2018

Abstract

IFN-induced protein with tetratricopeptide repeats 2 (IFIT2) plays important roles in host defense against viral infection as revealed by studies in humans and mice. However, little is known on porcine IFIT2 (pIFIT2). Here, we performed molecular cloning, expression profile, and transcriptional regulation analysis of *pIFIT2*. *pIFIT2* gene, located on chromosome 14, is composed of two exons and have a complete coding sequence of 1407 bp. The encoded polypeptide, 468 aa in length, has three tetratricopeptide repeat motifs. *pIFIT2* gene was unevenly distributed in all eleven tissues studied with the most abundance in spleen. Poly(I:C) treatment notably strongly upregulated the mRNA level and promoter activity of *pIFIT2* gene. Upstream sequence of 1759 bp from the start codon which was assigned +1 here has promoter activity, and deltaEF1 acts as transcription repressor through binding to sequences at position − 1774 to − 1764. Minimal promoter region exists within nucleotide position − 162 and − 126. Two adjacent interferon-stimulated response elements (ISREs) and two nuclear factor (NF)-κB binding sites were identified within position − 310 and − 126. The ISRE elements act alone and in synergy with the one closer to start codon having more strength, so do the NF-κB binding sites. Synergistic effect was also found between the ISRE and NF-κB binding sites. Additionally, a third ISRE element was identified within position − 1661 to − 1579. These findings will contribute to clarifying the antiviral effect and underlying mechanisms of *pIFIT2*.

Keywords Pig · IFIT2 · Cloning · Expression · Poly(I:C) · Promoter

Introduction

Host innate immune system secrets type I interferon (IFN) upon the detection of viruses, which, in turn, triggers the induction of hundreds of IFN-stimulated genes (ISGs). ISGs can block virus at multiple stages including modulation of viral entry into cells, translation initiation, propagation, and spread [1, 2]. Among the first ISGs to be discovered and cloned is the interferon-induced protein with tetratricopeptide repeats (IFITs) family composed of *IFIT*1, 2, 3, 5, and several pseudogenes and *IFIT-like* genes [3]. IFIT proteins are characterized by multiple repeats of tetratricopeptide repeat (TPR) helix-turn-helix motifs which are involved in numerous protein–protein interactions during various physiological and pathological process including translation initiation, cell migration, proliferation, double-stranded RNA signaling, and virus replication [4].

IFIT2, one of heavily studied family member, plays important roles in blocking viral infection. It is responsible for protecting mice from pathogenesis caused by the rhabdovirus Vesicular stomatitis virus [5, 6] and Rabies virus [7], the coronavirus mouse hepatitis virus [8], and the respirovirus Sendai virus [9]. Human IFIT2 is found to limit Hepatitis B virus replication in cultured cells [10]. It also restricts West Nile virus infection and pathogenesis in various human tissues in a cell type-specific manner, and contributes to the induction or magnitude of immune responses [11].

✉ Xiuqin Yang
xiuqin163@163.com; xiuqinyang@neau.edu.cn

✉ Di Liu
liudi1963@163.com

Xiaoyan Jing
xiaoyanjing373@sina.com

Yanfang Song
fushi66888@163.com

Caixia Zhang
zcx15663658352@163.com

[1] College of Animal Science and Technology, Northeast Agricultural University, Harbin 150030, China

[2] Agricultural Academy of Heilongjiang Province, Harbin 150086, China

The extensive antiviral effect of IFIT2 in human and mouse suggests its potential in protecting pig from viral disease. However, little is known on porcine *IFIT2* (*pIFIT2*). In the present work, we characterized the sequence, structure, and tissue expression profile of *pIFIT2* gene. To preliminarily explore its antiviral properties, in vitro experiments were conducted after treatment with viral analog, poly(I:C), a synthetic double-stranded RNA and has been extensively used to mimic viral infection [12, 13]. Moreover, the promoter activity and major *cis*-acting elements were identified as well. The results contribute to further revealing the antiviral effect and underlying mechanisms of *pIFIT2*, which will be helpful in breeding pigs with resistance to viral diseases.

Materials and methods

Animals, nucleotide acid isolation

Tissues including stomach, kidney, bladder, spleen, lung, heart, liver, large intestine, small intestine, muscle, and lymph were collected immediately after the pigs were slaughtered, snap frozen in liquid nitrogen and stored at − 70 °C. The protocol of animal treatment was according to the guidelines of the Ministry of Science and Technology of China [14]. Total RNA was isolated using TRIzol reagent (Invitrogen, Carlsbad, CA), treated with DNase I to remove the potential DNA contamination, and diluted into 1 μg/μl for future use. Genomic DNA was isolated from ear tissue using phenol/chloroform.

cDNA cloning

Based on EST, electronic sequences in pigs and orthologs in other species including human, mouse, dog, etc, one primer pair (Forward: 5′-aggaggatttctgaagagcac-3′; Reverse: 5′-atgttttgaataccaactcgg-3′) were designed for cloning porcine *IFIT2* cDNA. Reverse transcription (RT) was performed using PrimeScript® RT reagent kit (Perfect Real Time) (Takara, Dalian, China) with oligo(dT) primer and 1 μg total RNA as template. PCR reactions were conducted in a final volume of 25 μl containing 1×PCR buffer, 200 μM each dNTPs, 200 nM of each primer, 1 U Taq DNA polymerase (Takara), and 1 μl cDNA. PCR conditions were as follows, 95 °C for 5 min, followed by 30 cycles of 95 °C for 30 s, 58 °C for 30 s, 72 °C for 1 min, and 72 °C for 7 min. The PCR products were sub-cloned into pMD18-T (Takara) vector and sequenced by the Beijing Genomics Institute (BGI, Shenzhen, China). Sequence analysis was performed with the DNAMAN package (version 5.2.2) and the BLAST program at the National Center for Biotechnology Information (NCBI) website.

Real-time quantitative PCR

Expression profile of *pIFIT2* gene in tissues and that induced by poly(I:C) was analyzed using real-time quantitative PCR (qPCR). PK-15 cells were cultured as described previously [15] and stimulated with different poly(I:C) concentrations for 12 hours (h). cDNA from cells or tissues were synthesized as described above. qPCR was performed on Applied Biosystems 7500 instrument with SYBR *Premix Ex Taq*™ II (Takara) according to the manufacturer's protocol. Each reaction was run in 10 μl total volume in triplicate. The relative mRNA abundance of target genes was calculated using $2^{-\Delta\Delta C_t}$ method with β-actin as reference [16]. The primer pair for *pIFIT2* was as follows: Forward: 5′-gacggcagagaatgaaatgtg-3′; Reverse: 5′-gcaggcgagataggagcagac-3′.

Firefly luciferase reporter construct

Sequence between nucleotide (nt) position − 1838 and − 46 of *pIFIT2* gene was amplified from genomic DNA. The resulting products were first sub-cloned into pMD18-T (Takara) vector, and then ligated upstream of the firefly luciferase reporter gene in the pGL3-basic vector (Promega, Madison, WI) using the enzymes, *Kpn*I and *Xho*I, which were introduced into the end of products by primers. At the same time, a series of 5′ truncated fragments at nt position − 1759, − 1695, − 1661, − 1579, − 1499, − 1397, − 1146, − 894, − 654, − 389, − 310, − 225, − 162, and − 126 with a common 3′-terminus at − 46 bp were cloned into the pGL3-basic vector. In this report, the first nucleotide of coding sequence (CDS) was assigned position +1. Recombinant pGL3 plasmid obtained was named according to the name of forward primer used for amplification of inserted fragment, such as pGL3-A, pGL3-B, etc. The primers were given in Table 1.

Meanwhile, fragments absent of predicted deltaEF1 binding site, ISRE element, and NF-κB binding site were generated by overlap extension PCR as described previously [15]. Briefly, the deletion was first introduced into the ends of overlapping fragments by PCR with primers absent of the target site, respectively. And then the resulting products were spliced into a bigger one to introduce the deletion into the inner. The fragments obtained were inserted into the pGL3-basic vector (Promega), as described above, to construct mutant type reporter genes. All the reporter gene constructs were verified by DNA sequencing (BGI, Shenzhen, China). The primers used for

Table 1 Primers used for promoter analysis

Name	Sequence (5′–3′)	Position[a]
A-F	*GGTACC*TGCTGGTGGTTGATGACAATG	−1838
A1-F	GG*GGTACC*TCATCTCAGAGAATAGCAAG	−1759
A2-F	*GGTACC*GCCCATATTTTAGAACACAGAC	−1695
B-F	G*GGTACC*GTAATAAGCAGAGTAATCAGAAC	−1661
B1-F	GG*GGTACC*TTCCCAGTTTCTATTTTGC	−1579
B2-F	*GGTACC*GGACACATCATACACAGGC	−1499
C-F	*GGTACCC*TCCCCAGCCAGAACCTTTAT	−1397
D-F	GG*GGTACC*GACTATGTTTAGCCTACACTC	−1146
E-F	G*GGTACC*AGGAATGTTTGGCTTAGGTTAG	−894
F-F	G*GGTACC*GAATAAACTAAAGCAGGGAGAC	−654
G-F	G*GGTACC*GTGGTAAGGGTGGACAGAGT	−389
G1-F	*GGTACC*GTTGGGCTCCCTTGATG	−310
G2-F	C*GGTACC*TTGGCTCTTATTCAGCTCT	−225
G3-F	*GGTACC*AGTTTCAATTTCTCTTTCCTAAAGC	−162
G4-F	*GGTACC*AAGAAATCAGGTGCTGCC	−126
P-R	C*AAGCTT*CTACTGTGCTCTTCAGAAATCCTC	−46

F forward; *R* reverse. Endonuclease recognition sites were italicized

[a]Is the position of the first nucleotide in the promoter sequence in which "A" of the start codon was assigned position +1, the same as below

mutation were given in Table 2, and experiment project for site-directed deletion was given in Table 3.

Dual-luciferase reporter analysis

Each reporter gene construct was cotransfected into PK-15 cells with *Renilla* luciferase reporter plasmid (pRL-TK) (Promega, Madison, WI) using Lipofectamine 2000 reagent (Invitrogen) according to the manufacturer's protocol. At 24 h after transfection, the cells were collected and firefly and *Renilla* luciferase activities were measured with the Dual-Glo Luciferase Assay System (Promega). Relative luciferase activity was calculated as a ratio of firefly luciferase to *Renilla* luciferase. For poly(I:C) induction analysis, the cells were further treated in varied concentrations and time periods as indicated under "Results" before luciferase activity was measured.

Results

cDNA cloning and sequence analysis

The cDNA obtained was 1558 bp in length containing the complete CDS of 1407 bp, a 3′ untranslated region (UTR) of 80 bp, and a 5′ UTR of 71 bp. The sequence similarities of *pIFIT2* CDS with the homologs in human (NM_001547) and mouse (NM_008332.3) were 81.36 and 70.89%, respectively. Conceptual translation predicted that pIFIT2 protein, composed of 468 amino acids, had a theoretical molecular mass of 54 kDa and an isoelectric point of 6.92.

The *pIFIT2* gene was mapped to chromosome 14 using blat program (http://genome.ucsc.edu/cgi-bin/hgBlat). It is composed of two exons with the first one providing 5′ UTR and 5 nt of the CDS, and the second one containing the remaining part of the CDS and 3′ UTR. The gene structure of *pIFIT2* is identical to the homolog in human, somewhat different from murine *IFIT2* which has an extra short upstream exon (Fig. 1). A default motif search in SMART database (http://smart.embl-heidelberg.de/) revealed the presence of three TPR motifs in porcine and human IFIT2 proteins (Table 4), respectively, however no TPR was predicted in murine IFIT2 with the same method.

To gain insight of the evolutionary relationship between *pIFIT2* and the homologs in other vertebrates, a phylogenetic

Table 2 Primers used for site-directed mutation

Name	Sequence (5′–3′)	Position
deltaEF1-F	AACTGATGCAGCCCCTTCCTCATCT	−1789
deltaEF1-R	CTCTGAGATGAGGAAGGGGCTGCAT	−1749
ISREIII-F	CTCTCACTGAGTACATAGAAAACCGTTAGGAG	−1639
ISREIII-R	CCTAACGGTTTTCTATGTACTCAGTGAGAGTTC	−1596
ISREI-F	GAGTACTGCCAATTCACTTTCCTTTCCTAAAG	−184
ISREI-R	GCTTTAGGAAAGGAAAGTGAATTGGCAGTAC	−138
ISREII-F	AGAGTACTGCCAGTTTCAATTTCTCTTTCC	−185
ISREII-R	GGAAAGAGAAATTGAAACTGGCAGTACTCT	−144
DIS-F	AGAGTACTGCCTTTCCTAAAGCCTG	−185
DIS-R	ACAGGCTTTAGGAAAGGCAGTACTC	−134
NF-κBI-F	TCTTACTAAGATTAGAGTACTGCC	−209
NF-κBI-R	GGCAGTACTCTAATCTTAGTAAGAGCTG	−175
NF-κBII-F	CTCCCTTGATGGCAGAAAGAAATTCTAACTC	−303
NF-κBII-R	GAATTTCTTTCTGCCATCAAGGGAGCCC	−268

Table 3 Experiment project for element deletion in overlap extension PCR

Elements	PCR 1	PCR 2	PCR 3	Splicing PCR
ΔdeltaEF1	A-F/deltaEF1-R	deltaEF1-F/P-R		A-F/P-R
ΔISREIII	A-F/ISREIII-R	ISREIII-F/P-R		B-F/P-R
ΔISREI	G-F/ISREI-R	ISREI-F/P-R		G1-F/P-R
ΔISREII	G-F/ISREII-R	ISREII-F/P-R		G1-F/P-R
ΔISREI-II	G-F/DIS-R	DIS-F/P-R		G1-F/P-R
ΔNF-κBI	G-F/NF-κBI-R	NF-κBI-F/P-R		G1-F/P-R
ΔNF-κBII	G-F/NF-κBII-R	NF-κBII-F/P-R		G1-F/P-R
ΔNF-κBI-II	G-F/NF-κBII-R	NF-κBII-F/NF-κBI-R	NF-κBI-F/P-R	G1-F/P-R
ΔNF-κBI + ISREI-II	G-F/NF-κBI-R	NF-κBI-F/DIS-R	DIS-F/P-R	G1-F/P-R
ΔNF-κBII + ISREI-II	G-F/NF-κBII-R	NF-κBII-F/DIS-R	DIS-F/P-R	G1-F/P-R
ΔNF-κBI-II + ISREI-II	G-F/DIS-R	DIS-F/P-R		G1-F/P-R

ISREI-II and NF-κBI-II indicate double deletion of ISREs and NF-κB binding sites, respectively, while NF-κBI-II + ISREI-II indicates that two ISRE elements and two NF-κB binding sites were deleted simultaneously. In regular PCRs 1, 2, and 3, cloning plasmid containing fragment from −1838 to −45 of *pIFIT2* gene was used as template except for deleting NF-κBI-II + ISREI-II in which PCR products having NF-κBI-II deletion was used as template; in the following splicing PCRs, products of PCRs 1, 2 and 3, if have, were mixed equally and used as template

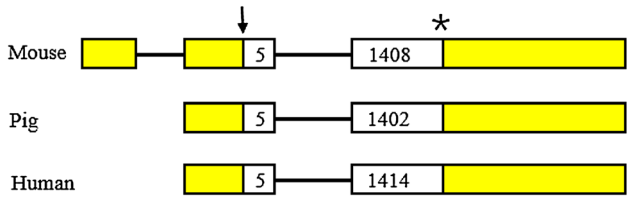

Fig. 1 Genomic structure of IFIT2 orthologs among mouse, pig and human. Boxed regions are exons connected by introns that are indicated with lines. Shading represents untranslated region. Arrow and asterisk indicates position of start and stop codon, respectively. Numbers are the length of coding sequence

tree was constructed (Fig. 2). We found that *IFIT2* gene only exists in mammals. The ancient *IFIT2* gene originated from sorex and was divided into four subgroups, Rodentia A, Insectivora B, Rodentia B, and Insectivora C/Chiroptera. Rodentia B is the ancestor of euarchontoglires to which human being belongs, while Insectivora C/Chiroptera is the ancestor of laurasiatheria to which pig belongs. The evolution of *IFIT2* gene in euarchontoglires and laurasiatheria tends to stable. The phylogenetic relationship revealed by the tree topology conforms to the taxonomic classification of the species used. The sequences have been submitted to the GenBank database under Accession No. JX070559.

Expression profiles

pIFIT2 gene was ubiquitously expressed in all 11 tissues analyzed with the most abundance in spleen, followed by liver, and heart. In the remaining tissues, including lung, kidney, stomach, muscle, lymph, large intestine, and small intestine, the relative mRNA level was much lower with the least abundance in bladder (Fig. 3).

The kinetics of transcriptional induction of *pIFIT2* gene in response to poly(I:C) were analyzed with pGL3-B construct. The induction was in a time- and dose-dependent manner. The best induction time was for 8–12 h and the promoter activity was dropped when the time was for 24 h (Fig. 4a). Therefore, 12 h was used as induction time in the following experiments. The promoter activity was increased with the increasing of poly(I:C) concentration. It was induced slightly when the concentration was from 0.5 to 5 ng/ml, and sharply at a concentration of 10 ng/ml (Fig. 4b). At the same time, the response of endogenous *pIFIT2* gene to poly(I:C) was measured with RT-qPCR method in PK-15 cells, and the similar results was obtained (Fig. 4c).

Table 4 Distribution of TPR motifs in IFIT2 from pig and human

Name	Species	GenBank No.	Polypetide length	TPR 1[a]	TPR 2[a]	TPR 3[a]
Pig	*Sus scrofa*	JX_070559	468	51–84	94–127	243–276
Human	*Homo sapiens*	NM_001547	472	51–84	172–208	247–280

[a]Position of TPR motifs in the polypetide

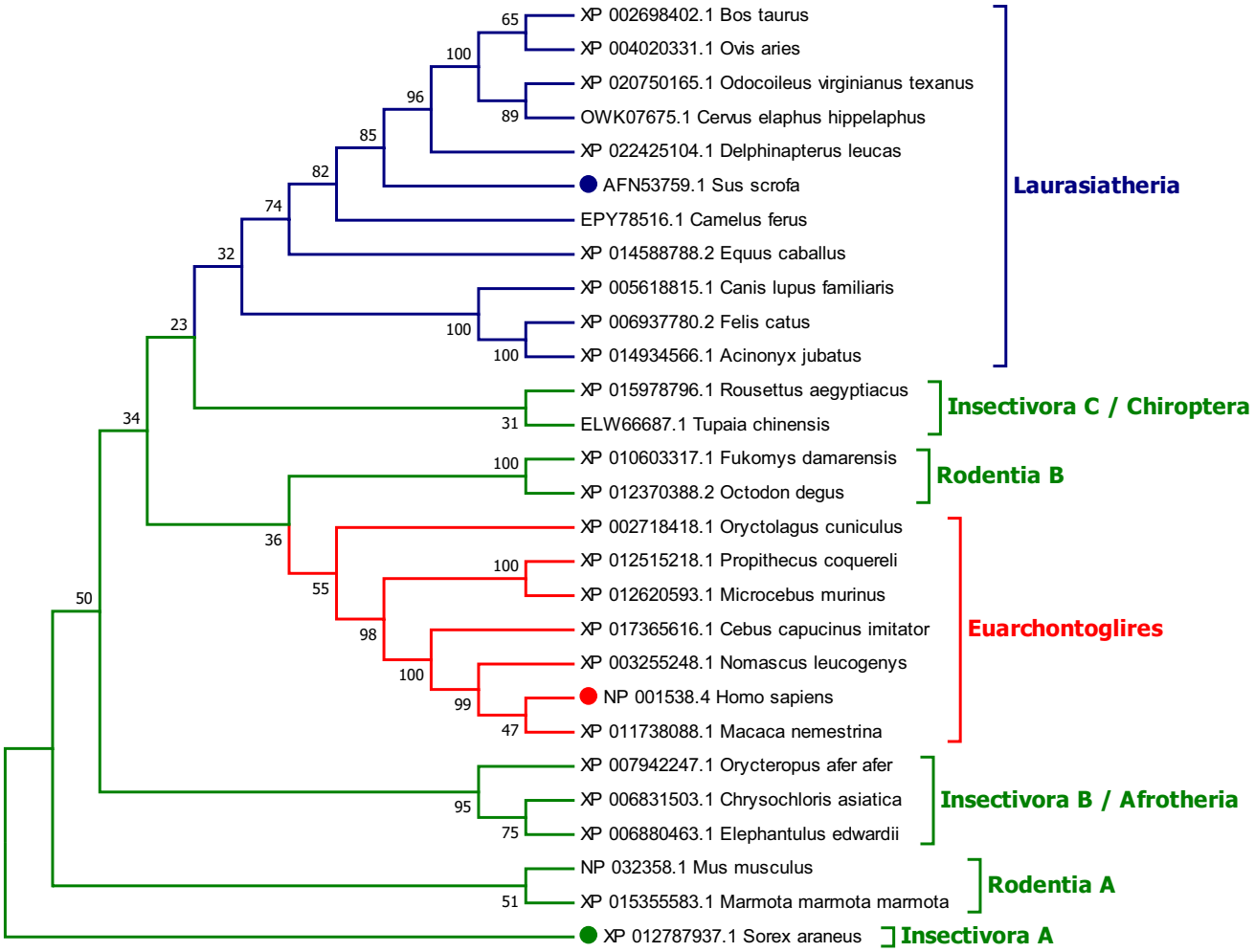

Fig. 2 Evolutionary relationships of *IFIT2* gene. The evolutionary history was inferred using the Neighbor-Joining method. The bootstrap consensus tree inferred from 500 replicates is taken to represent the evolutionary history of the taxa analyzed. Branches corresponding to partitions reproduced in less than 50% bootstrap replicates are collapsed. The percentage of replicate trees in which the associated taxa clustered together in the bootstrap test (500 replicates) are shown next to the branches. The evolutionary distances were computed using the Poisson correction method and are in the units of the number of amino acid substitutions per site. The analysis involved 28 amino acid sequences. All positions containing gaps and missing data were eliminated. There were a total of 361 positions in the final dataset. Evolutionary analyses were conducted in MEGA7

Promoter identification

We transfected a series of luciferase reporter gene constructs containing *pIFIT2* gene upstream region into PK-15 cells (Fig. 5a). The results showed that the construct pGL3-B directs highest level luciferase expression, while construct pGL3-A has little promoter activity. Also evident, the construct pGL3-G directs above background level luciferase expression. Additionally, significant difference in luciferase expression level was observed between the constructs pGL3-B and pGL3-C. These data indicate that there are basal promoter region between nt position − 389 and − 45, positive regulatory element between − 1661 and − 1397, and potent repressive element within − 1838 to − 1661.

Further analysis narrows the repressive element to nt position − 1838 to − 1759 and the positive regulatory regions to − 1661 to − 1579 (Fig. 5b, c). Additionally, significant differences in luciferase expression level were observed between constructs pGL3-G and pGL3-G1, pGL3-G1 and pGL3-G2, and between pGL3-G2 and pGL3-G3. No luciferase activity was measured for construct pGL3-G4. These data indicate that regulatory elements exist within the nt positions − 389 and − 126, and that the minimal promoter region exists within position − 162 and − 126 (Fig. 5d).

Identification of the major regulatory element

Using online program TFSEARCH (http://www.cbrc.jp/research/db/TFSEARCH.html) and Alibaba 2 (http://

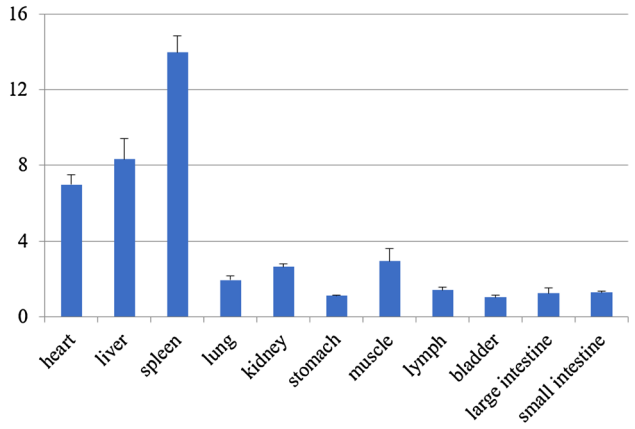

Fig. 3 Tissue expression profile of porcine *IFIT2* gene. The relative expression level in bladder was used as 1. Each column represents the mean ± SE of triplicate determinations

www.gene-regulation.com/pub/programs/alibaba2/index.html), five sequence motifs, including two consecutive ISREs and nuclear factor (NF)-κB binding sites located at position − 310 to − 126, and another ISRE at position − 1661 to − 1579, were identified (Fig. 6). ISREI motif exactly matches the consensus sequence, 5′-AGTTTC NNTTTC(C/T)-3′, whereas ISREII and ISREIII diverge at a few nucleotide positions. Additionally, one deltaEF1 binding sequence was present at position − 1774 to − 1764.

To test the functional significance of the candidate *cis*-acting elements we prepared mutant type reporter constructs with the sequences deleted. A total of one pGL3-A mutant, one pGL3-B mutant, and nine pGL3-G1 mutants were obtained. In each modified construct, the whole candidate sequence was deleted. DeltaEF1 binding site deletion restored the promoter activity strongly (Fig. 6a). The promoter activity of construct deleting ISREIII was 33.76% compared to its wild type counterpart (Fig. 6b).

The two ISRE motifs at position − 310 to − 126 acts alone and in synergy to activate the promoter activity, so do the NF-κB binding sites. The promoter activity was decreased strongly in the absence of ISREI (12.72% compared to the wild type counterpart) or ISREII (55.04%). The deletion of both elements produced a synergistic response in that only 3.89% activity was found compared to the wild type counterpart. Similarly, the promoter activity was decreased with the deletion of NF-κBI (35.3%) or NF-κBII binding site (53.81%), and synergistic response (21.7%) existed in double deletion. Synergistic effects were also found between ISRE and NF-κB binding sites: when one of the NF-κB binding site and both ISRE elements were deleted simultaneously, the activity was only 1.94% (NF-κBI and both ISRE deleting) and 2.78% (NF-κBII and both ISRE deleting), respectively, compared to the wild type construct; when the four motifs at the

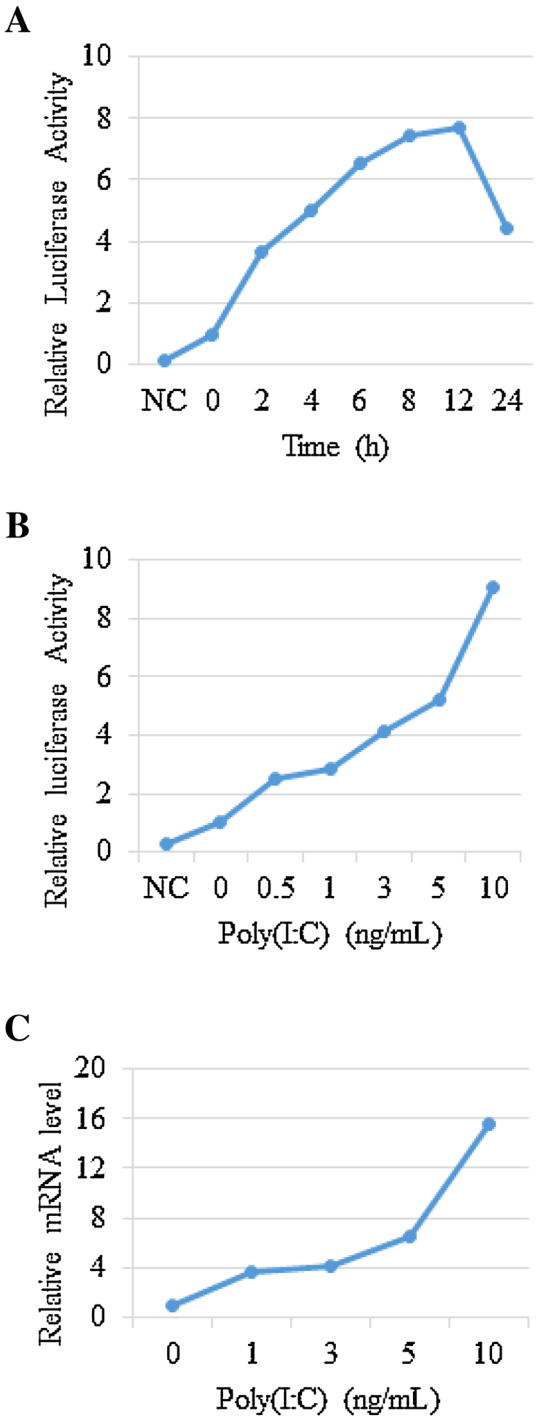

Fig. 4 Induction kinetics of *pIFIT2* by poly(I:C). PK-15 cells were induced with 10 ng/ml poly(I:C) for different time periods (**a**) or with different concentrations of poly(I:C) for 12 h (**b**) after transiently transfected with promoter construct pGL3-B for 24 h. The relative luciferase activity is displayed relative to the non-treatment control, which was used as 1. **c** Induction of endogenous *pIFIT2* by poly(I:C). PK-15 cells were induced by poly(I:C) for 12 h. The relative mRNA level is measured with RT-qPCR method and displayed relative to the non-treatment control, which was used as 1. Data are representative of three individual experiments, each with three replicates. Each column represents the mean ± SE

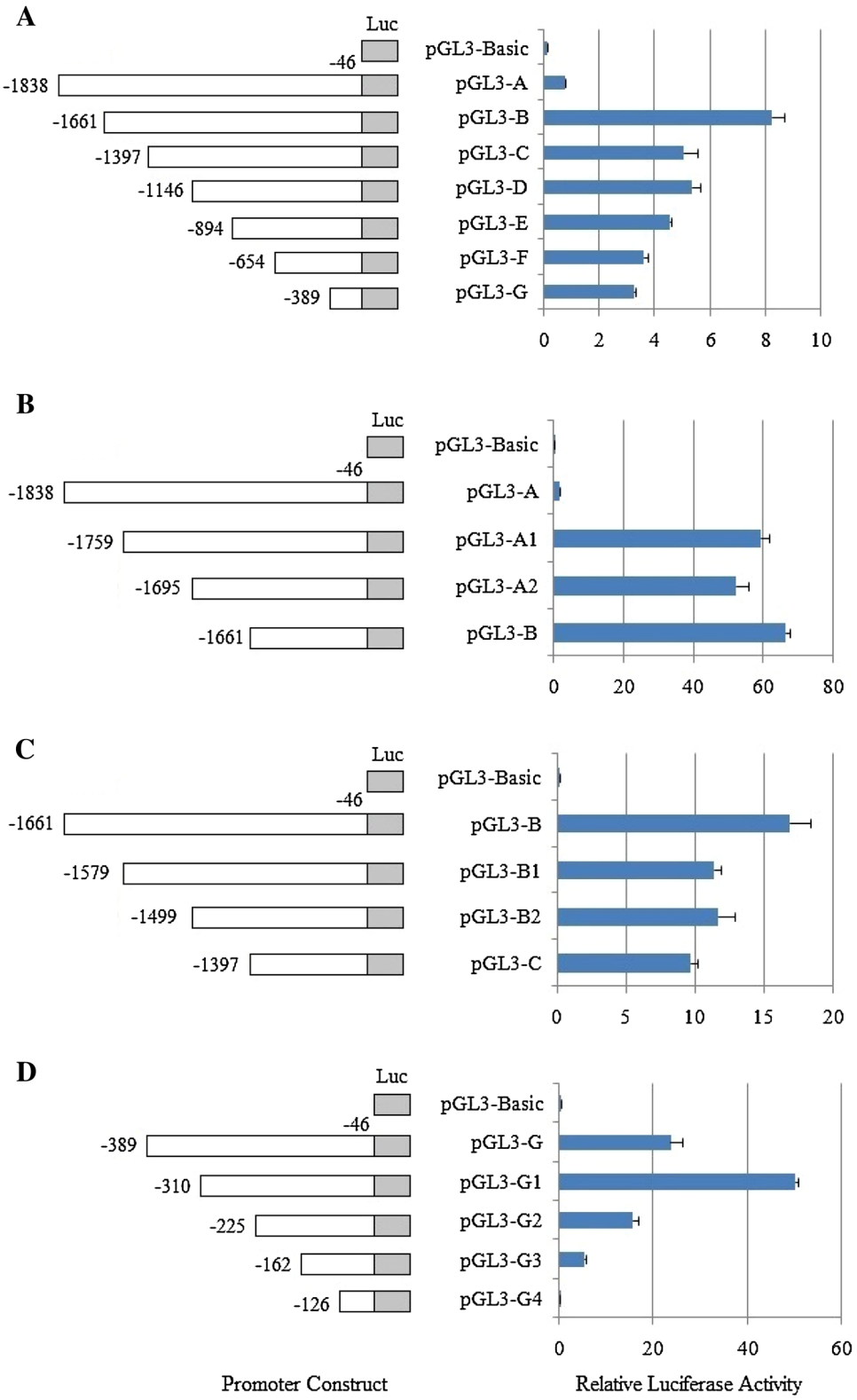

Fig. 5 Identification of important region for transcriptional activation of *pIFIT2*. Data are representative of three individual experiments, each with three replicates. Each column represents the mean ± SE

region were deleted simultaneously, the promoter was almost completely inactivated (Fig. 6c).

Deleting ISRE and/or NF-κB binding sites caused a strong decrease of poly(I:C)-induced promoter activity. The induction of pGL3-B construct deleting ISREIII by poly(I:C) was 71% compared to the wild type control. The promoter induction was also strongly reduced with the deletion of ISREI (28% compared to the wild type counterpart)

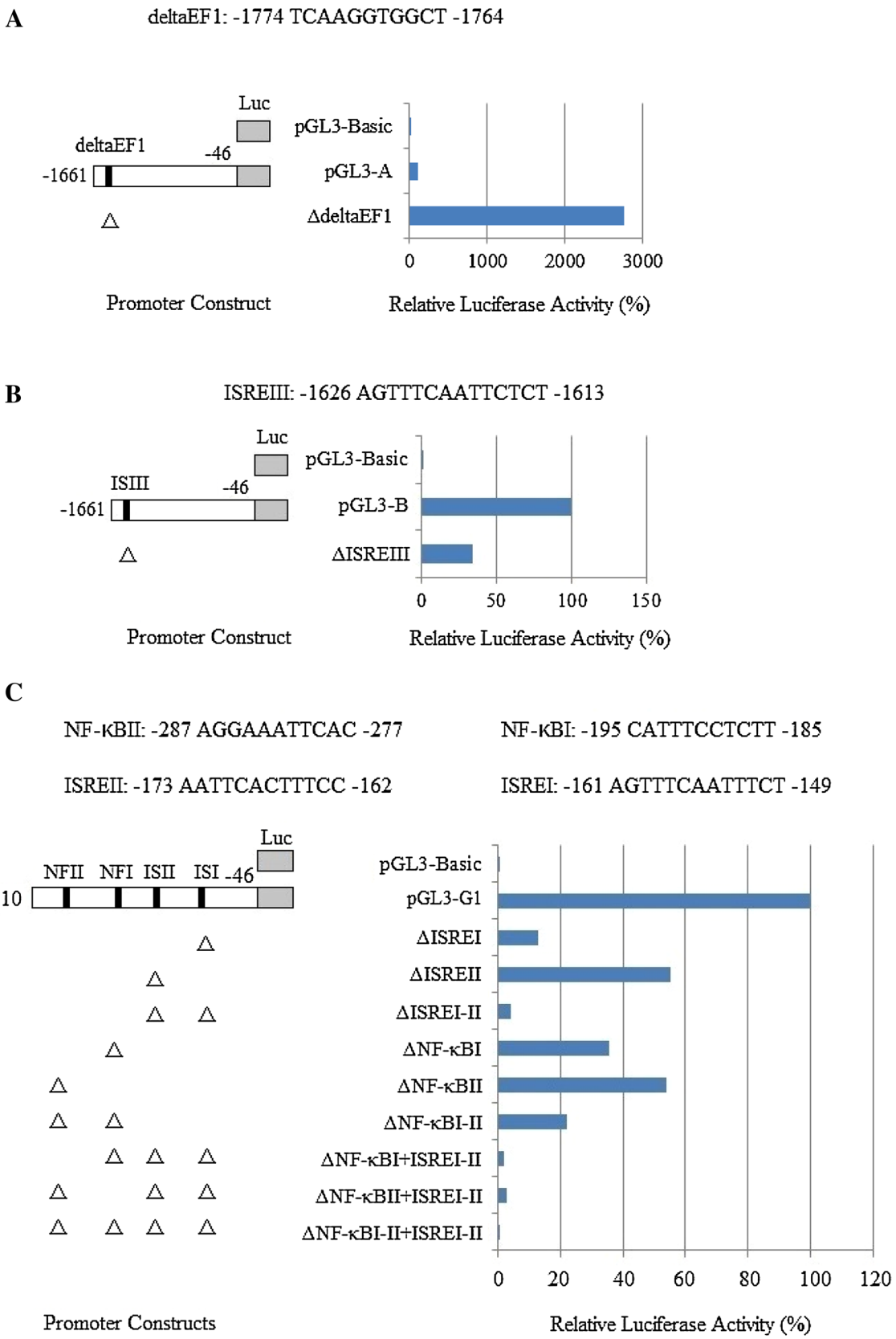
A
deltaEF1: -1774 TCAAGGTGGCT -1764
Luc
deltaEF1
-46
-1661
pGL3-Basic
pGL3-A
ΔdeltaEF1
0
1000
2000
3000
Promoter Construct
Relative Luciferase Activity (%)
B
ISREIII: -1626 AGTTTCAATTCTCT -1613
Luc
ISIII
-46
-1661
pGL3-Basic
pGL3-B
ΔISREIII
0
50
100
150
Promoter Construct
Relative Luciferase Activity (%)
C
NF-κBII: -287 AGGAAATTCAC -277
NF-κBI: -195 CATTTCCTCTT -185
ISREII: -173 AATTCACTTTCC -162
ISREI: -161 AGTTTCAATTTCT -149
Luc
NFII NFI ISII ISI -46
-310
pGL3-Basic
pGL3-G1
ΔISREI
ΔISREII
ΔISREI-II
ΔNF-κBI
ΔNF-κBII
ΔNF-κBI-II
ΔNF-κBI+ISREI-II
ΔNF-κBII+ISREI-II
ΔNF-κBI-II+ISREI-II
0
20
40
60
80
100
120
Promoter Constructs
Relative Luciferase Activity (%)

◂**Fig. 6** Identification of major *cis*-acting elements of *pIFIT2* promoter. Δ indicates that the corresponding element is deleted. IS and NF represent ISRE element and NF-κB binding site, respectively. The relative luciferase activity is displayed relative to the wild-type construct, pGL3-A, pGL3-B or pGL3-G1, which was used as 100%. Data are representative of three individual experiments, each with three replicates. Each column represents the mean ± SE

or ISREII (52%). Similarly, pGL3-G1 construct absent of NF-κBI or NF-κBII binding site showed a strong decrease in transcriptional response to poly(I:C), as well: the induction was 38 and 65%, respectively, compared to the wild type counterpart. The synergistic effects were also found between both ISRE elements or NF-κB binding sites. When the four motifs in the region were deleted simultaneously, the promoter was hardly response to poly(I:C) (Fig. 7).

Discussion

Porcine *IFIT2* should be an important molecule in innate antiviral immune responses, as revealed by studies in human and mice. Elucidation of its role and regulatory mechanism underlying expression and activation will contribute to preventing viral infection and pathogenesis in pigs, and to breeding pigs resistant to viral diseases. Here the existence of *pIFIT2* gene is confirmed using molecular biology techniques for the first time, and its expression profile in tissues and that induced by poly(I:C) was characterized. Additionally, the transcriptional regulation of *pIFIT2* gene was analyzed, which revealed major *cis*-acting elements including three ISREs, two NF-κB, and one deltaEF1 binding sites existed in the promoter.

There are four *IFIT* genes, *IFIT1/2/3/5*, in human, while mice are absent of *IFIT5*. These molecules are similar but distinct in structure [17, 18]. We showed that *pIFIT2* has the same structure as its counterpart in human: both of them are composed of two exons and have three confidently predicted TPR motifs. The sequence similarity of *IFIT2* between human and pig is high (81.36 and 72.30% at the CDS and amino acid level, respectively). Additionally, phylogenetic analysis, revealed an evolutionary relationship among mammals. These data provide an evidence that *IFIT2* is evolutionally conserved. Sequence and structure are the basis for the function of a given gene. We thus expect similar roles of *pIFIT2* gene in viral infection and pathogenesis in pigs.

RT-qPCR revealed that *pIFIT2* transcripts were present in all tissues studied with different amounts. The expression of murine *IFIT2* is strongly induced in response to type I IFNs, poly(I:C), and infection by a lot of viruses, while in untreated tissues including spleen, lung, kidney, liver, colon, and small intestine, it is undetectable or detectable at very low levels with western blotting method [18]. Also, there are no detectable levels of *IFIT* mRNA in untreated HT1080 cells and HEK293 cells using RNase protection assay [17]. The sensitivity of the methods used may be the reason for the differences between our results and others. The *pIFIT2* is induced by poly(I:C) in a time- and dose-dependent manner, and the induction pattern is similar to that of human *IFIT2* gene whose mRNA level is induced strongly by poly(I:C) at 6 h, remained constant at 12 h, and dropped sharply between 12 and 24 h in HT1080 cells [17]. Studies have shown that *IFIT* genes are regulated in a cell type-, inducer-, and gene-specific manner [18–20]. These results indicate that *pIFIT2* is highly regulated and might have similar role in viral defense to that of homolog in human.

The upstream sequence of the *pIFIT2* can drive the expression of firefly luciferase, while the strength can be repressed almost completely if a 79 bp region (positions − 1838 to − 1759) further upstream is included (up to position − 1838). This indicates that the upstream region corresponds to a functional promoter, and that a potent repressive element exists between positions − 1838 and − 1759. Bioinformatic analysis has revealed common consensus sequence for transcription factor deltaEF1 between positions − 1838 and − 1759. DeltaEF1 factor, a zinc finger protein, is implicated in the regulation of a lot of viral and cellular genes with functionally diverse roles [21, 22]. Through binding directly to the promoters, it represses transcription of epithelial splicing regulatory protein 2 [23], E-cadherin [24] and Plakophilin 3 genes [25], and suppresses promoter activity of chicken infectious anemia virus [26] as well. Here, we confirmed that deltaEF1 is also transcription repressor of *pIFIT2* gene. Additionally, the promoter activity was strongly enhanced when the fragment was truncated from nt position − 389 to − 310 at the 5′ end, indicating another repressor present here. No specific transcription factor binding site was predicted in the region using TFSEARCH program, while by using Alibaba 2 program, Id3 consensus sequence was identified. Id3 is a dominant-negative regulator of transcription by sequestering other TFs, thus making them unable to bind DNA [27, 28]. However, the promoter activity was not restored when the predicted motif was deleted partially or completely from construct pGL3-G (data not given). The results reveal that Id3 is not involved in the transcription of *pIFIT2*, and there should be other factors regulating *pIFIT2* expression.

The ISRE is essential for IFN inducibility of ISGs. Here, we confirmed that there are two adjacent ISREs in *pIFIT2*, as its counterparts in human and mouse [17, 18]. These two elements act synergistically with ISREI, closer to the start codon, having more strength. Furthermore, a third functional ISRE element was identified in the upstream of *pIFIT2* promoter. To our knowledge, this is not reported previously for other *IFIT* promoters. As we use different reporter genes to confirm the potential elements, ISREIII and ISREI-II, we cannot reveal which one is the strongest in the induction

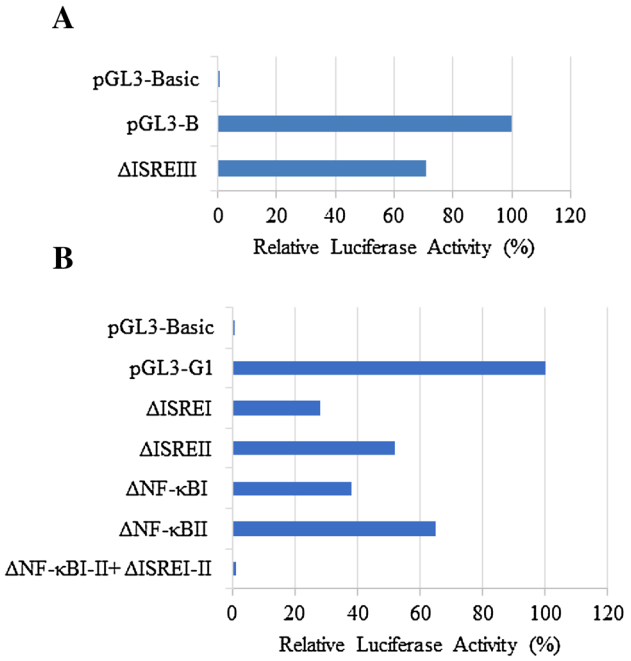

Fig. 7 Effects of *cis*-acting elements on poly(I:C) induction. PK-15 cells were induced with 10 ng/ml poly(I:C) for another 12 h after transfected with reporter gene for 24 h. The relative luciferase activity is displayed relative to the non-treatment control, which was used as 100%

of *pIFIT2*. However, we assure *pIFIT2* is more sensitive to poly(I:C). Here, we show that 10 ng/ml poly(I:C) can induce the expression of *pIFIT2* effectively, while in a simultaneously performed experiment we found that 50 ng/ml poly(I:C) induce activity of *pIFIT5* promoter marginally (data not given), and that efficient induction of *pIFIT5* need a μg/ml level of poly(I:C) concentration [29]. This may be correlated with the existence of ISREIII.

The role of ISRE motif in the transcriptional activation of ISGs is critical and well documented, while other transcription factors involved in regulating ISG expression remain to be clarified. NF-κB, a transcription factor family including p50, p52, p65/RelA, RelB, c-Rel, and v-Rel, regulates the expression of genes involved in antiviral immune response by binding to *cis*-acting sites in the promoters. The induction of murine *Ifit1* and *Isg15* was lower by type I IFN in NF-κB knock out fibroblasts than in wild-type cells, while the induction of *Mx1* and *Nmi* was at much higher levels, indicating that NF-κB plays a selective and distinct role in regulating the expression of ISGs and the induction of antiviral activity [30]. Further analysis revealed that p50 directly binds to the promoter of *Mx1* gene and thereby refrains its induction [31]. We demonstrated here that NF-κB binding sites play a positive role in the activation of *pIFIT2*, which is similar to the effects of NF-κB on *Ifit1* and *Isg15* induction. Further experiment needs to be performed to identify which member of NF-κB family binding to the *cis*-acting element. Nevertheless, we identified several important *cis*-acting elements in the promoter region of *pIFIT2*, which will contribute to clarifying the mechanism underlying its transcriptional regulation.

Acknowledgements This work was supported by the Scientific Research Foundation of Heilongjiang Provincial Education Department (12541014) and Foundation for Improving Innovative Capability of Scientific Institutions, Heilongjiang (YC2016D001).

Compliance with ethical standards

Conflict of interest The authors declare that they have no conflict of interest.

References

1. Sadler AJ, Williams BR (2008) Interferon-inducible antiviral effectors. Nat Rev Immunol 8(7):559–568
2. Schoggins JW, Rice CM (2011) Interferon-stimulated genes and their antiviral effector functions. Curr Opin Virol 1(6):519–525
3. Zhou X, Michal JJ, Zhang L, Ding B, Lunney JK, Liu B, Jiang Z (2013) Interferon induced IFIT family genes in host antiviral defense. Int J Biol Sci 9(2):200–208
4. D'Andrea LD, Regan L (2003) TPR proteins: the versatile helix. Trends Biochem Sci 28(12):655–662
5. Fensterl V, Wetzel JL, Ramachandran S, Ogino T, Stohlman SA, Bergmann CC, Diamond MS, Virgin HW, Sen GC (2012) Interferon-induced Ifit2/ISG54 protects mice from lethal VSV neuropathogenesis. PLoS Pathog 8(5):e1002712
6. Fensterl V, Wetzel JL1, Sen GC (2014) Interferon-induced protein Ifit2 protects mice from infection of the peripheral nervous system by vesicular stomatitis virus. J Virol 88(18):10303–10311
7. Davis BM, Fensterl V, Lawrence TM, Hudacek AW, Sen GC, Schnell MJ (2017) Ifit2 is a restriction factor in rabies virus pathogenicity. J Virol 91(17):e00889-17
8. Butchi NB, Hinton DR, Stohlman SA, Kapil P, Fensterl V, Sen GC, Bergmann CC (2014) Ifit2 deficiency results in uncontrolled neurotropic coronavirus replication and enhanced encephalitis via impaired alpha/beta interferon induction in macrophages. J Virol 88(2):1051–1064
9. Wetzel JL, Fensterl V, Sen GC (2014) Sendai virus pathogenesis in mice is prevented by Ifit2 and exacerbated by interferon. J Virol 88(23):13593–13601
10. Pei R, Qin B, Zhang X, Zhu W, Kemper T, Ma Z, Trippler M, Schlaak J, Chen X, Lu M (2014) Interferon-induced proteins with tetratricopeptide repeats 1 and 2 are cellular factors that limit hepatitis B virus replication. J Innate Immun 6(2):182–191
11. Cho H, Shrestha B, Sen GC, Diamond MS (2013) A role for Ifit2 in restricting West Nile virus infection in the brain. J Virol 87(15):8363–8371
12. Weber F, Wagner V, Rasmussen SB, Hartmann R, Paludan SR (2006) Double-stranded RNA is produced by positive-strand RNA viruses and DNA viruses but not in detectable amounts by negative-strand RNA viruses. J Virol 80(10):5059–5064
13. Wang L, Wang JK, Han LX, Zhuo JS, Du X, Liu D, Yang XQ (2017) Characterization of miRNAs involved in response to poly(I:C) in porcine airway epithelial cells. Anim Genet 48(2):182–190
14. Ministry of Science and Technology of China (2006) Guidelines on humane treatment of laboratory animals ([2006] 398). http://

www.most.gov.cn/fggw/zfwj/zfwj2006/200609/t20060930_54389.htm. Accessed 30 Sept 2006
15. Li HT, Liu D, Yang XQ (2011) Identification and functional analysis of a novel single nucleotide polymorphism (SNP) in the porcine Toll-like receptor (TLR) 5 gene. Acta Agric Scand Sect A 61(4):161–167
16. Livak KJ, Schmittgen TD (2001) Analysis of relative gene expression data using real-time quantitative PCR and the $2^{-\Delta\Delta C_t}$ method. Methods 25:402–408
17. Terenzi F, Hui DJ, Merrick WC, Sen GC (2006) Distinct induction patterns and functions of two closely related interferon-inducible human genes, ISG54 and ISG56. J Biol Chem 281(45):34064–34071
18. Terenzi F, White C, Pal S, Williams BR, Sen GC (2007) Tissue-specific and inducer-specific differential induction of ISG56 and ISG54 in mice. J Virol 81:8656–8665
19. Wacher C, Müller M, Hofer MJ, Getts DR, Zabaras R, Ousman SS, Terenzi F, Sen GC, King NJ, Campbell IL (2007) Coordinated regulation and widespread cellular expression of interferon-stimulated genes (ISG) ISG-49, ISG-54, and ISG-56 in the central nervous system after infection with distinct viruses. J Virol 81:860–871
20. Fensterl V, White CL, Yamashita M, Sen GC (2008) Novel characteristics of the function and induction of murine p56 family proteins. J Virol 82:11045–11053
21. Flanagan JR, Becker KG, Ennist DL, Gleason SL, Driggers PH, Levi BZ, Appella E, Ozato K (1992) Cloning of a negative transcription factor that binds to the upstream conserved region of Moloney murine leukemia virus. Mol Cell Biol 12:38–44
22. Park K, Atchison ML (1991) Isolation of a candidate repressor/activator, NF-E1 (YY-1, delta), that binds to the immunoglobulin kappa 3′ enhancer and the immunoglobulin heavy-chain mu E1 site. Proc Natl Acad Sci USA 88:9804–9808
23. Horiguchi K, Sakamoto K, Koinuma D, Semba K, Inoue A, Inoue S, Fujii H, Yamaguchi A, Miyazawa K, Miyazono K, Saitoh M (2012) TGF-β drives epithelial-mesenchymal transition through δEF1-mediated downregulation of ESRP. Oncogene 31(26):3190–3201
24. Eger A, Aigner K, Sonderegger S, Dampier B, Oehler S, Schreiber M, Berx G, Cano A, Beug H, Foisner R (2005) DeltaEF1 is a transcriptional repressor of E-cadherin and regulates epithelial plasticity in breast cancer cells. Oncogene 24(14):2375–2385
25. Aigner K, Descovich L, Mikula M, Sultan A, Dampier B, Bonné S, van Roy F, Mikulits W, Schreiber M, Brabletz T, Sommergruber W, Schweifer N, Wernitznig A, Beug H, Foisner R, Eger A (2007) The transcription factor ZEB1 (deltaEF1) represses Plakophilin 3 during human cancer progression. FEBS Lett 581(8):1617–1624
26. Miller MM, Jarosinski KW, Schat KA (2008) Negative modulation of the chicken infectious anemia virus promoter by COUP-TF1 and an E box-like element at the transcription start site binding deltaEF1. J Gen Virol 89(Pt 12):2998–3003
27. Jen Y, Weintraub H, Benezra R (1992) Overexpression of Id protein inhibits the muscle differentiation program: in vivo association of Id with E2A proteins. Genes Dev 6:1466–1479
28. Norton JD, Deed RW, Craggs G, Sablitzky F (1998) Id helix-loop-helix proteins in cell growth and differentiation. Trends Cell Biol 8:58–65
29. Zhang J, Shao SY, Li LZ, Liu D, Yang XQ (2015) Molecular cloning and characterization of porcine interferon-induced protein with tetratricopeptide repeats (IFIT) 5. Can J Anim Sci 95(4):551–556
30. Pfeffer LM, Kim JG, Pfeffer SR, Carrigan DJ, Baker DP, Wei L, Homayouni R (2004) Role of nuclear factor-kappaB in the antiviral action of interferon and interferon-regulated gene expression. J Biol Chem 279(30):31304–31311
31. Wei L, Sandbulte MR, Thomas PG, Webby RJ, Homayouni R, Pfeffer LM (2006) NFkappaB negatively regulates interferon-induced gene expression and anti-influenza activity. J Biol Chem 281(17):11678–11684